

## Messier 3: A Deep Dive

PATRICK COSTA<sup>1</sup> AND ADDISON DESALVO, ABBAS JAFFERY, WARREN UTSCHINSKI<sup>1</sup>

<sup>1</sup> University of Washington Astronomy Department

### ABSTRACT

We set out to estimate the age of Messier 3 by constructing a color-magnitude diagram and identifying the main-sequence turnoff point. After remotely collecting data using the 0.5m FlareCam telescope at the Astrophysical Research Consortium Small Aperture Telescope, we used calibration frames to correct our images of Messier 3 and several photometric-standard stars. We used the data from the standard stars along with the photutils Python package to model the relationship between pixel value and flux with the intention of applying our model to the Messier 3 data. Our model proved incorrect and ineffective and we were left to try other methods of constructing a color-magnitude diagram, but to no avail. We were unable to accomplish our goal of estimating the age of Messier 3, which is known to be around 12 Gyr.

### 1. INTRODUCTION

On the nights of May 4 and May 5, we remotely connected to the Astrophysical Research Consortium Small Aperture Telescope (ARCSAT) at Apache Point Observatory (APO) in Sunspot, New Mexico. We used their 0.5m telescope, FlareCam, to take images of Messier 3 (M3), a globular cluster in the Canes Venatici constellation. In section 2, we will discuss the process of collecting data with ARCSAT. A globular cluster is a spherical collection of stars bound together by gravity. Stars in these clusters are typically around the same age, so knowing the age of one star is a good estimate for the age of the entire population. The age of the cluster can be estimated by the main sequence turnoff point on a color-magnitude diagram of the population. A color-magnitude diagram can be made from pictures taken of a cluster in two different bandwidth filters. In section 3 we discuss data reduction and how we constructed a color-magnitude diagram for M3 from our data. We chose to take pictures of M3 in particular because of its visibility during our observing window and the fact that other astronomers have already made color-magnitude diagrams of it and estimated its age, so we would be able to compare our results to theirs. A discussion of our results and how they compare to previous results can be found in section 4. We also took pictures of 10 photometric-standard stars. Photometric-standard stars are stars with known brightnesses. We took images of these stars with the purpose of modeling a relationship between the measured flux and the known apparent magnitude. We then planned on applying that model to the data taken of M3 to calculate the apparent magnitudes of the stars in the population from the fluxes we measured. We would then have the necessary information to construct a color-magnitude diagram.

### 2. METHODS

We connected to ARCSAT remotely by tunneling into APO to access the telescope control software. After connecting, we took calibration frames. First, we took 11 bias frames, then 5 dark frames. Bias frames are 0 second exposures taken with the shutter of the telescope closed. They reveal the CCD's intrinsic dark fixed-pattern noise that must be subtracted from subsequent images. The dark frames we took had 3 minute exposure times because the longest exposure time we took of M3 was 3 minutes. Dark current is caused by the thermal excitation of electrons that occurs during exposures when the CCD warms up. Dark frames isolate the noise associated with dark current. Next, we took 3 flat frames each in the B-band and V-band. Flat frames fully illuminate the CCD and demonstrate the variability in responsiveness for each pixel. Figure 1 shows calibration images of all 3 types. The bias frame included shows minor noise, while the dark frame shows greater noise caused by dark current. The flat frame shows the high variability from pixel to pixel. For every image of M3 taken, the noise and variable responsiveness revealed by the calibration frames are present. As further discussed in the next section, we had to correct each image of M3 for these intrinsic sources of error.

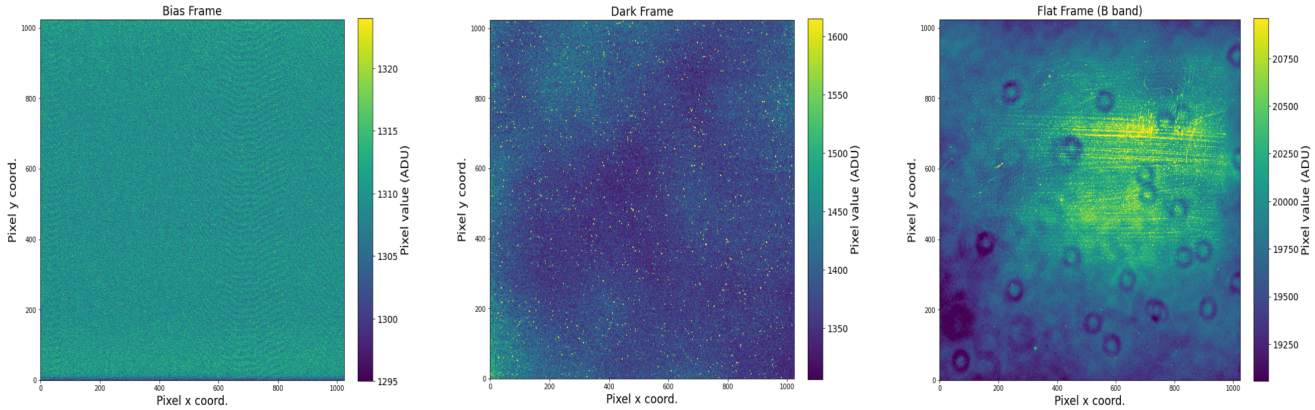


**Figure 1.** (Left to right) A bias frame, dark frame, and flat frame taken with FlareCam. The x- and y-axes are the dimensions of the 1024x1024 pixel CCD. The colorbar to the right of each plot shows a gradient between the maximum and minimum pixel values (ADU) in each frame.

After taking all of our calibration frames, we used ARCSAT’s SkyCam to check for clouds above the telescope and saw quite a few. We waited for about an hour for the weather to clear up before taking images of M3 in the B and V bands. We chose to take images with the Johnson-Cousins B and V band filters because of their popularity and they were recommended by our supervisor, Sarah Tuttle. First, we took 20 second exposures of M3 in the B and V bands. We chose 20 seconds as our first exposure time because we thought that it would be a good middle ground in terms of not over-exposing the center of the cluster so much so that we would not be able to distinguish between stars near the center, and not under-exposing the stars farther from the center. By the end of our first observing night, we also took 60, 90, 120, and 180 second exposures in both bands. We chose these exposure times because the stars farther from the center became more visible, so we could get a better understanding of the population of the cluster.

On the second observing night, we again had to wait close to an hour for the weather to cooperate. This time, there were no visible clouds, but sensors told us that the concentration of dust particles was too high for data to be taken. Once the dust subsided, we took shorter exposures of 3, 5, and 10 seconds in both bands to get clearer images of the stars closer to the center of the cluster. After taking all of these images, we realized that there was an “Auto-focus” option in the telescope software, so we re-took all of our exposures including those taken the night prior with auto-focusing on with the thought that our images would be clearer, which turned out to be the case. Having clear images of long and short exposures would allow us to better identify sources both close and far from the center of the cluster.

Next, our supervisor, Bo-Eun Choi, suggested that we take images of photometric-standard stars so we could calculate the apparent magnitude of the stars in M3. Ideally there would be a standard star in the same frame as our images of M3, but unfortunately this was not the case. Using a list of standard stars from Landolt (2009), we took images of 10 stars that were at right ascensions close to that of M3, 13h 42m 11.62s. Airmass is dependent on RA, with lower RA having more airmass because there is more atmosphere between the observer and the object being observed, and measurements such as flux can differ depending on airmass. Therefore, we wanted to be looking through airmass close to the same as we did for M3. The standard stars we imaged with 10 second exposures and their relevant data are shown in Figure 2.

### 3. ANALYSIS AND RESULTS

#### 3.1. Reduction Procedures

After collecting all of our desired data, we set out to create a color-magnitude diagram. The first step was to correct all images using the biases, darks, and flats we took. We averaged each set of calibration frames such that we had a master bias, master dark, a master flat in the B band, and a master flat in the V band. Then, we subtracted the master bias and master dark from every image of M3 and standard stars. We then flat corrected every image using the master flat in the same band as each image. Lastly, we used the photutils Python package to estimate and subtract the sky background from every image. For example, Figure 3 shows the result of the calibration process for the 90 second exposure of M3 in the B band with auto-focusing active.

Star Designation	RA	Dec	V	B-V
105505	13:35:24	-00:23:47	10.27	1.422
105815	13:40:04	-00:02:19	11.453	0.385
106700	14:40:51	-00:23:50	9.785	1.362
121968	13:58:51	-02:55:38	10.254	-0.186
+2 2711	13:42:20	+01:29:58	10.367	-0.166
105437	13:37:17	-00:38:05	12.535	0.248
104485	12:44:23	-00:30:20	15.017	0.838
104479	12:43:55	-00:32:55	16.087	1.271
PG1407-013	14:10:26	-01:30:16	13.75	-0.259

**Figure 2.** Table of photometric-standard stars imaged. Shows each star’s designation, RA, Dec, apparent V magnitude, and B-V color index (Landolt 2009).

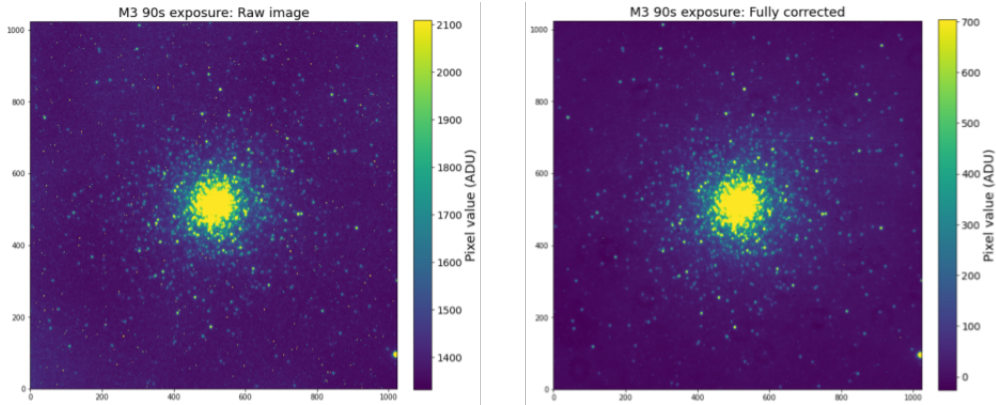


**Figure 3.** Left: Raw image taken of M3 with a 90 second exposure in the B band and auto-focus turned on. Right: Image of M3 after subtracting the master bias, dark, flat, and sky background.

### 3.2. Source Detection

Next, we were interested in the relationship between the pixel values of sources and their fluxes. We set out to find a model relating the two that we could use to calculate the flux of the sources found in M3. To do this, we used DAOStarFinder to detect sources in the images of the standard stars. DAOStarFinder returns a table with, most notably, all of the sources detected and their positions, pixel values, and fluxes. In every image, we detected more than one source, so we had to determine which source was the standard star. More often than not, this was a simple task as the standard star was the closest to the middle of the image because FlareCam centers on the object we set it to image. There were some cases, though, where we could not identify which source was the standard star. For example, Figure 4 shows the image taken of +2 2711 in the B band. There are two sources detected near the center of the image and we could not determine which was the standard star, so we omitted +2 2711 from our analysis. Notice in Figure 4 how DAOStarFinder has detected two sources overlapping each other, depicted by the overlapping red circles. This was the case for several other images, leaving us to choose which source detection was more likely to be true. Such choices were almost completely arbitrary, but in some cases one detected source had an incredibly high peak pixel value and we chose to discard it and use the other detected source. The lack of rhyme or reason in our decisions in overlapping scenarios undoubtedly presents itself as a significant source of error.

After looking at the images and determining which sources were the standard stars, we plotted the relationship between their flux and peak pixel value. We then used `numpy.polyfit` to calculate a linear model of the relationship. For the B band, our model yielded:  $F = 0.02132P - 1.274$  where  $F$  is the flux and  $P$  is the peak pixel value, while in the V band, we modeled:  $F = 0.01935P - 3.239$ . To determine whether or not our models were accurate, we had to determine if DAOStarFinder accurately measured flux. We calculated the B-V color index by using equation (1)

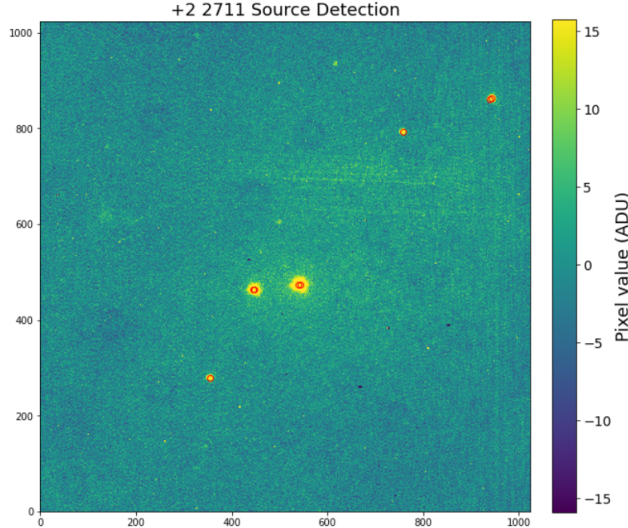


**Figure 4.** Image taken of +2 2711 in the B band. The red circles are the detected sources. We could not determine which of the sources in the middle of the image

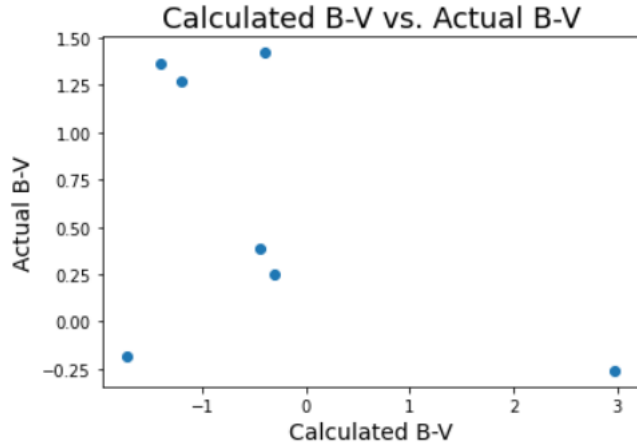


**Figure 5.** A scatter plot of our calculated B-V compared to the actual B-V given by Landolt (2009). As is clear, there was no relationship between the two.

and compared our values to those given in Figure 2. We found that none of our calculated values matched those from Landolt (2009), so we plotted our calculated values against the actual values to see if there was any relationship. Unfortunately, as shown in Figure 5, there was no visible correlation between them.

$$m_b - m_v = 2.5 \log_{10} \left( \frac{F_v}{F_b} \right) \quad (1)$$

Due to the inaccuracy of the flux calculations by DAOStarFinder, we discarded our flux vs. peak pixel value model. Had we more time, we would have tried to use make a Point Spread Function (PSF) model and use it to perform PSF photometry with DAOPhotPSFPhotometry.

Next, we used DAOStarFinder to detect sources in our images of M3. For each image, we set the minimum and maximum peak pixel values such that we would not detect any sources in the center of cluster or any very faint sources likely not part of the cluster. We did not want DAOStarFinder to detect sources in the center of the cluster because we our images were clearly oversaturated in the center, making it highly unlikely any source detection there would be accurate. For example, Figure 6 shows the 90 second exposure of M3 with the source detections indicated by the

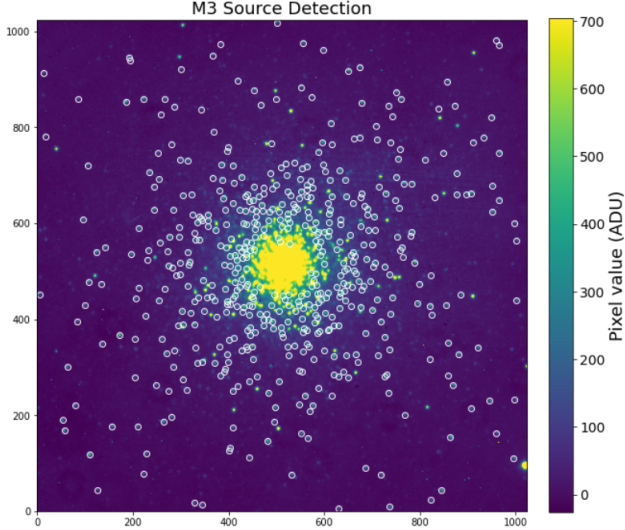


**Figure 6.** 90 second exposure of M3. The white circles indicate the position of the detected sources. The minimum threshold for detection was 200 ADU and the maximum was 700 ADU.

white circles. We did not want DAOStarFinder to detect very faint sources because it was unlikely such sources would be part of the cluster. They would be more likely to be beyond the cluster.

### 3.3. Color-magnitude diagram

After detecting sources in all of our images of M3, we wanted to calculate the B-V color indices for all of the sources. Considering the inaccuracy of our peak vs. flux model, we instead planned to calculate the B-V color index by subtracting each source's V magnitude from their B magnitude. In the table returned by our source detection, there was a column of magnitudes, although considering the inaccurate measurement of fluxes, the magnitude measurements were likely inaccurate as well. We decided that time constraints prevented us from finding a better way to calculate the magnitudes, so we used those calculated by DAOStarFinder. The use of those magnitudes introduced significant error.

Furthermore, DAOStarFinder did not detect the same sources in the B and V bands of each exposure time, and in the cases it did, they were rarely detected in the same order. This made it so we could not make the assumption that the  $i$ 'th source in the B table was the same as the  $i$ 'th source in the V table. Without realizing the now-known lack of consistency in our source detection, we tried to simply subtract the V magnitude from the B magnitude for every source, but ran into the first problem that the number of sources detected differed between the bands.

We then made the assumption that the sources were detected in the same order up until the point where the number of detections in one band exceeded those in the other. For example, we detected 518 sources in the 90 second exposure in the B band, and 478 for the same exposure in the V band, so we used only the first 478 sources from the B band. Figure 7 shows the result of this assumption. After realizing this assumption was incorrect, we tried to formulate a way to determine common sources detected in both bands for the same exposure time. At first, we considered writing a function that would look for common x and y coordinates of sources in both tables to within a few pixels, but we predicted this method would not yield a favorable result due to how close the sources are to each other. However, we thought it was worth a try. Figure 8 shows the result of this method applied to the same 90 second exposures used in Figure 7. As expected, Figure 8 does not resemble a color-magnitude diagram.

Our final method of creating a color-magnitude diagram for M3 was repeating the method behind Figure 8, but extending it to every image we took of M3. We wanted to determine common sources across every image and then take the average B and V magnitudes to make a color-magnitude diagram. Unfortunately, we reached the limits of our Python abilities and were left with Figure 8 as our final result.

## 4. DISCUSSION

Our goal was to construct a color-magnitude diagram and identify the main-sequence turnoff point to estimate the age of the cluster. Compared to the color-magnitude diagrams of M3 derived by others (see Buonanno et al.

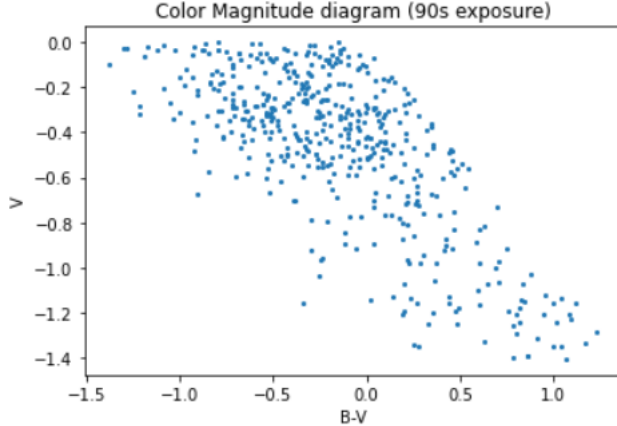


**Figure 7.** B-V vs. V for sources detected from 90s exposures of M3. The B and V magnitudes are not associated with the same sources as per the incorrect assumption that the sources were detected in the same order.

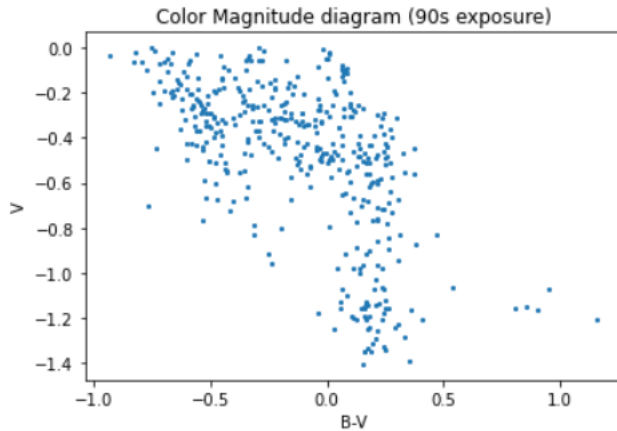


**Figure 8.** B-V vs. V for sources detected from 90s exposures of M3. Unlike Figure 7, this figure's B and V magnitudes are associated with common sources. Sources were considered common across bands if they were detected within 5 pixels of each other.

(1994), Sandage (1953), and Massari et al. (2016)), ours is not what one would expect to calculate from the data we took. As previously discussed, a plethora of significant sources of errors along with limited knowledge of Python packages including photutils played important roles in our miscalculation. Unfortunately our miscalculation of the color-magnitude diagram prevented us from completing our goal of estimating M3's age, which is estimated to be around 12 Gyr (Wenger & Buser 2003).

Along the way, though, much was learned about the importance of calibration frames, photometric-standard stars, and photometry. Calibration frames are necessary when taking any data with a telescope because of the intrinsic noise of the telescope and CCD. Standard stars are important because they act as reference points for calculating the flux of other stars. Photometry done correctly also aids in the calculation of the flux of sources. We also learned that stars in globular clusters, especially those in M3, can be hard to distinguish from one another because of how close they are to each other.

## REFERENCES

Buonanno, R., Corsi, C. E., Buzzoni, A., et al. 1994, A&A, 290, 69  
 Landolt, A. U. 2009, AJ, 137, 4186,  
 doi: [10.1088/0004-6256/137/5/4186](https://doi.org/10.1088/0004-6256/137/5/4186)

Massari, D., Lapenna, E., Bragaglia, A., et al. 2016,  
 MNRAS, 458, 4162, doi: [10.1093/mnras/stw583](https://doi.org/10.1093/mnras/stw583)  
 Sandage, A. R. 1953, AJ, 58, 61, doi: [10.1086/106822](https://doi.org/10.1086/106822)

Wenger, E., & Buser, R. 2003, in Astronomical Society of the Pacific Conference Series, Vol. 296, New Horizons in Globular Cluster Astronomy, ed. G. Piotto, G. Meylan, S. G. Djorgovski, & M. Riello, 406